

Theoretical Review of Charmonium Production with Different p_T in the Hot Medium

Baoyi Chen^{1,2,*} and Carsten Greiner^{2,**}

¹Department of Physics, Tianjin University, Tianjin 300350, China

²Institut für Theoretische Physik, Goethe-Universität Frankfurt, Max-von-Laue-Str. 1, D-60438 Frankfurt am Main, Germany

Abstract. Charmonia with different transverse momentum p_T usually comes from different mechanisms in the relativistic heavy ion collisions. This work tries to review the theoretical studies on quarkonium evolutions in the deconfined medium produced in p-Pb and Pb-Pb collisions. The charmonia with high p_T are mainly from the initial hadronic collisions, and therefore sensitive to the initial energy density of the bulk medium. For those charmonia within $0.1 < p_T < 5$ GeV/c at the energies of Large Hadron Collisions (LHC), they are mainly produced by the recombination of charm and anti-charm quarks in the medium. In the extremely low $p_T \sim 1/R_A$ (R_A is the nuclear radius), additional contribution from the coherent interactions between electromagnetic fields generated by one nucleus and the target nucleus plays a non-negligible role in the J/ψ production even in semi-central Pb-Pb collisions.

1 Introduction

Since charmonium abnormal suppression proposed as one of the signals of the deconfined medium produced in nucleus-nucleus (AA) collisions [1], abundant theoretical studies [2–8] about charmonium evolutions in hot medium have been done to reveal different aspects of heavy quark (HQ) interactions with the bulk medium. This paper briefly lay out theoretical models and compare them with the experimental data, trying to give a full picture of charmonium evolutions in the hot medium. Heavy quark interactions inside $c\bar{c}$ can be partially screened by the thermal partons with color charges [9]. As the heavy quark interactions at large distance are screened at first, charmonium states (J/ψ , χ_c , $\psi(2S)$) with different geometry sizes are sequentially melt as the medium temperature increases [10]. Close to the critical temperature T_c of the deconfined phase transition, J/ψ wave function is less modified by the thermal medium compared with the excited states. The medium-induced large decay rate suppresses the production of excited states and also J/ψ total production, as $\sim 40\%$ of the final J/ψ come from the decay of excited states (χ_c , $\psi(2S)$) in heavy ion collisions [11]. Nuclear modification factor R_{AA} , defined as the ratio of charmonium yield in nucleus-nucleus (AA) collisions $N_{AA}^{J/\psi}$ and the production in proton-proton (pp) collisions scaled by the number of binary collisions N_{coll}^{pp} , measures the magnitude of hot medium effects on charmonia. The deviation of R_{AA} from unit is due to the parton inelastic scatterings and color screening effects.

*e-mail: baoyi.chen@tju.edu.cn

**e-mail: carsten.greiner@th.physik.uni-frankfurt.de

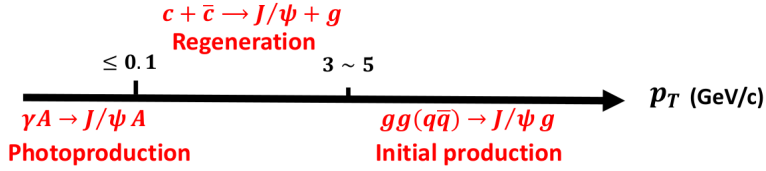


Figure 1. Schematic figure for charmonium initial production, regeneration, coherent photoproduction dominated in different transverse momentum p_T . The figure is cited from [12].

With only primordial production, J/ψ nuclear modification factor R_{AA} should decrease with the colliding energies $\sqrt{s_{NN}}$ where hotter medium medium is expected in the larger $\sqrt{s_{NN}}$. However, from Relativistic Heavy Ion Collider (RHIC) to the Large Hadron Collider (LHC), colliding energy increases about 10 times, but the J/ψ nuclear modification factor is enhanced instead of being suppressed [13, 14]. Besides, this enhancement is only located in the small transverse momentum region. This phenomena is now well clarified by the regeneration mechanism [15], where single charm and anti-charm quark from different pairs can combine into a new charmonium during the QGP expansion, due to the large binding energy of J/ψ in the thermal medium. This process happens after the primordial production. Charmonium yield from regeneration process is proportional to the densities of charm and anti-charm quark $\rho_{c(\bar{c})}(t, \mathbf{r}, \mathbf{p}_{c(\bar{c})})$ and also the cross section of the reaction $c + \bar{c} \rightarrow J/\psi + g$ [16]. As the cross section of charm pair $\sigma_{pp}^{c\bar{c}}$ increases significantly with $\sqrt{s_{NN}}$, abundant charm pairs at LHC energies can significantly enhance the regeneration process and the R_{AA} . Different from color singlet bound state, single charm quarks carry color charges and are strongly coupled with QGP. This is supported by the observables of open charm mesons such as elliptic flows of D mesons and its nuclear modification factor [17]. With strong energy loss of heavy quarks in the thermal medium [18], the regenerated charmonia tend to carry small momentum compared with the primordially produced charmonia. Assuming charm quarks reach kinetic equilibrium in their momentum distribution, one can roughly obtain the mean transverse momentum of the regenerated charmonia $\langle p_T^\Psi \rangle \sim 2p_c \sim 4T_{QGP}$. At RHIC and LHC Pb-Pb collisions, QGP typical temperature in the most phase space (not the initial maximum temperature) is around $T_{QGP} \sim 200 - 300$ MeV, which results in $\langle p_T^\Psi \rangle \sim 1$ GeV/c for regenerated charmonium. It is below the mean transverse momentum of the primordially produced charmonia $2 \sim 3$ GeV/c. As charm quarks are strongly coupled with the anisotropic medium, they also carry the momentum anisotropies due to the different accelerations of QGP expansion in the transverse plane. This will also be inherited to the final charmonium observables [19, 20].

In the semi-central collisions, there are hadronic collisions in the overlap area of two nuclei. Meanwhile, nucleus with large electric charges carried by protons moves with nearly the speed of light $v_N = \sqrt{E_N^2 - m_N^2}/E_N > 0.999c$ at RHIC and the LHC energies with the relation $E_N = \sqrt{s_{NN}}/2$. The strong electromagnetic (EM) pulse from the moving protons can not only change charged/chiral particle evolutions such as Chiral Magnetic Effect (CME) [21], etc, but also interact with the target nucleus to generate new particles called photoproduction [12, 22]. This has been widely studied in Ultra-peripheral collisions absent of hadronic collisions, and are expected to be negligible with the existence of QGP. However, both recent experimental and theoretical studies indicate that this photoproduction can be several times larger than the contribution from hadronic collisions, but only in the extremely low transverse momentum region $p_T \sim 1/R_A < 0.1$ GeV/c [23]. These photoproduced charmonia from EM fields will

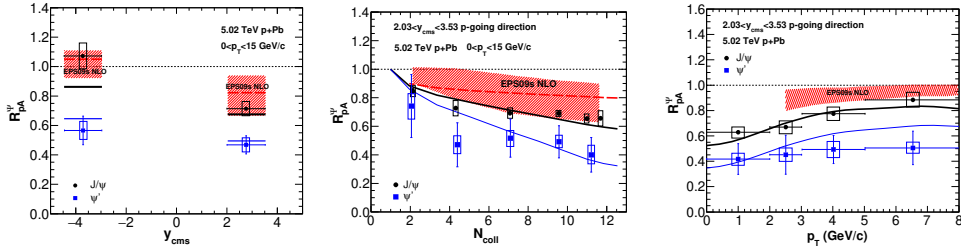


Figure 2. (Color online) J/ψ and $\psi(2S)$ nuclear modification factors as a function of rapidity, number of binary collisions (centralities), transverse momentum respectively at $\sqrt{s_{NN}} = 5.02$ TeV p-Pb collisions. The band only includes shadowing effects. Lines are the full calculations with both cold and hot medium effects for J/ψ and $\psi(2S)$. These figures are cited from [24].

also suffer hot medium dissociations generated by the hadronic collisions, and in turn gives more constraints on the magnitude of the EM fields and EM-induced particle evolutions.

2 Charmonium from primordial production, regeneration and photoproduction

Charmonium production from hadronic collisions and the QGP modifications can be well described with microscopic transport models. Extensive theoretical and experimental studies indicate multiple mechanisms contributing to the final charmonium yield, each of them dominant in different p_T bins see Fig.1. Focus on the primordial production at first, we present charmonium evolutions in p-Pb collisions, where regeneration process is suppressed due to the small number of charm pairs in QGP.

2.1 primordial production and the hot medium effects in pA collisions

We study the nuclear modification factors of different charmonium states which suffer similar cold nuclear matter effects (such as shadowing effect on the parton densities in the nucleus) but different final state interactions. The heavy quark pairs are produced almost instantly at $\tau < 1/(2m_c)$ where m_c is the mass of charm quark. Neglect charmonium formation process and assume the heavy quark pair can evolve into a certain eigenstate before the time scale $\tau_0 \sim 0.6$ fm/c of QGP reaching local equilibrium, one can simulate the evolutions of charmonium density in phase space in $\tau \geq \tau_0$ with the transport model [12],

$$p^\mu \partial_\mu f_\Psi = -C_\Psi f_\Psi + \beta_\Psi \quad (1)$$

here f_Ψ is the charmonium phase space density, and C_Ψ is the decay rate caused by hot medium interactions including parton inelastic scatterings and color screening. β_Ψ will be zero when absent of regeneration. Different final state interactions for J/ψ and $\psi(2S)$ are embodied in the factor C_Ψ . In the hot medium produced in p-Pb collisions, both initial energy density and the geometry size of QGP is relatively small compared with Pb-Pb collisions. J/ψ eigenstate can survive from this hot spot, but $\psi(2S)$ suffer non-negligible dissociations from the deconfined medium. This makes $R_{AA}^{\psi(2S)}$ becomes smaller than $R_{AA}^{J/\psi}$ in different rapidities, centralities and the momentum bin, see Fig.2. The model of ‘‘similar cold nuclear matter effects + different QGP suppressions’’ can explain well $R_{AA}^{J/\psi}$ and $R_{AA}^{\psi(2S)}$ in the forward rapidity [24]. In the backward rapidity defined as Pb-going direction where hotter medium

is expected, anti-shadowing effect can enhance the J/ψ and $\psi(2S)$ yields at the same time. With only shadowing effect from EPS09 NLO model [25], both J/ψ and $\psi(2S)$ R_{AA} is around ~ 1.1 . However, experimental data of $R_{AA}^{\psi(2S)}$ in the backward rapidity is only 0.3 in the central collisions with $N_{coll} \sim 11$. After including the hot medium suppressions, $R_{AA}^{\psi(2S)}$ from the transport model is close to the experimental data, but $R_{AA}^{J/\psi}$ is also suppressed to 0.8 below the experimental data, see Fig.3. This result is consistent with the transport model developed by TAMU Group [26]. Note that the calculations from Comover model seem to be closer to the experimental data (~ 0.95 in the central collisions) [27] as they employ a larger anti-shadowing effect which can enhance both J/ψ and $\psi(2S)$ yields. We can obtain similar results if employing a larger anti-shadowing factor as an input of the transport model. Another possible explanation for Fig.3, is that $\psi(2S)$ transit into J/ψ with in-medium HQ potential instead of being dissociated. As at $T \sim T_c$, HQ potential from Lattice QCD calculations is restored at the distance of J/ψ mean radius, but is still screened at the distance of $\psi(2S)$ radius. This partially screened in-medium HQ potential can result in transition of $\psi(2S) \leftrightarrow J/\psi$, and change the relation between $R_{AA}^{J/\psi}$ and $R_{AA}^{\psi(2S)}$ [28].

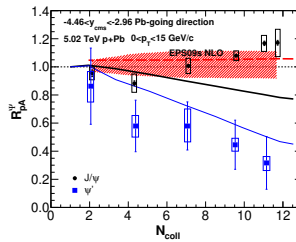


Figure 3. J/ψ and $\psi(2S)$ nuclear modification factor as a function of the number of binary collisions in the backward rapidity at $\sqrt{s_{NN}} = 5.02$ TeV p-Pb collisions. The figure is cited from [24].

2.2 sequential regeneration and the charm quark diffusion

In the Pb-Pb collisions at LHC energies, QGP can dissociate most of the primordially produced charmonia. The regeneration becomes dominant in the low p_T region. The process of charm quark energy loss and the momentum thermalization in QGP can be studied with Langevin equation, transport models, etc. In the limit of kinetic thermalization, charm quark spatial densities will be diluted by the expansion of the bulk medium [29]. In the early stage of QGP expansion, charmonium regeneration is difficult to happen due to the strong color screening on HQ potential. Regenerated charmonia can only survive in the later stage of QGP expansions when in-medium heavy quark potential is partially restored. In higher colliding energies with larger QGP initial temperature, hot medium takes longer to cool down and regenerate charmonia. That means, charm quarks in the expanding QGP will be “blown” outside and their spatial densities is relatively suppressed. Meanwhile, the regenerated charmonia will carry larger collective flows and larger momentum [19].

In order to see the charm quark diffusion effect on regenerated charmonia, one can focus on the observable $N_{AA}^{J/\psi} / (N_c)^2$ (here N_c represents charm quark number in AA collisions). It describes the probability of one charm combining with another anti-charm quark to generate J/ψ . This observable does not depend on the shadowing effect and the charm pair cross section $\sigma_{pp}^{c\bar{c}}$. Its value is mainly determined by the evolutions of charm quark density and the recombination rate. In the left panel of Fig.4, from semi-central to central collisions, the

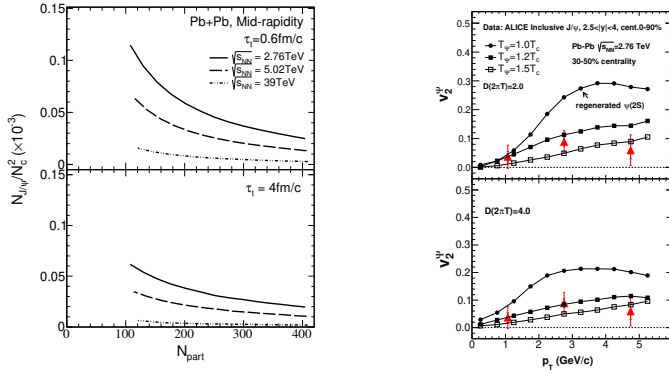


Figure 4. The left panel is $N_{J/\psi}/(N_c)^2$ as a function of number of participants N_p with the assumption of charm quark reaching kinetic equilibrium at different time τ_f , here N_c represents equals the number of all charmed particles. The right panel is the elliptic flow of regenerated charmonia at different temperature. It is simulated by the Langevin equation. These figures are cited from [19, 29].

initial temperature of QGP increases which results in stronger diffusions of charm quarks in the QGP. From $\sqrt{s_{NN}} = 2.76$ TeV to 39 TeV, the value of $N_{AA}^{J/\psi}/(N_c)^2$ decreases with $\sqrt{s_{NN}}$. This charm diffusion effect is also reflected in the comparison of J/ψ and $\psi(2S)$. As J/ψ and $\psi(2S)$ are thermally produced in the different stages of QGP expansion due to different binding energies, charm quarks can inherit larger collective flows from the anisotropic bulk medium which will also be inherited to the regenerated $\psi(2S)$ [16]. In the right panel of Fig.4, with the model consisting of ‘‘Langevin equation for charm evolution + coalescence mechanism for charm hadronization’’ [19, 30], elliptic flow of regenerated $\psi(2S)$ is always larger than the value of regenerated J/ψ .

2.3 photoproduction in extremely low p_T

Nucleus moves with nearly the speed of light to generate electromagnetic pulse in the relativistic heavy ion collisions. This electromagnetic field interacts with the other nucleus to produce vector mesons or dileptons. The photoproduction, however, was believed to be negligible compared with the contribution of hadronic collisions. Therefore, the photoproduction has been widely studied only in Ultra-peripheral collisions where photoproduction becomes the only source for particle production [22, 31–34]. Now, we find that photoproduction is also visible in the semi-central collisions but only in $p_T < 0.1$ GeV/c.

Instead of dealing with the interactions between electromagnetic fields (generated by one nucleus) and the other nucleus, one can approximate this Lorentz-contracted EM fields to be longitudinally moving quasi-real photons, see Eq.(2) [35]. The longitudinal direction is defined as the beam direction. This quasi-real photons can scatter with the nucleus to fluctuate into a certain vector meson such as ϕ , J/ψ , $\psi(2S)$, etc, see Eq.(3) and the left panel of Fig.5. As photons interact with the target nucleus coherently, the typical transverse momentum of the produced particle is $p_T \sim 1/R_A$,

$$\int d\tau \int d\mathbf{x}_T \cdot (\mathbf{E}_T \times \mathbf{B}_T) = \int d\omega w \frac{dN_\gamma}{d\omega} \quad (2)$$

$$\frac{d\sigma_{AA \rightarrow AA J/\psi}}{dy}(y) = \frac{dN_\gamma}{dy}(y) \sigma_{\gamma A \rightarrow A J/\psi}(y) + \frac{dN_\gamma}{dy}(-y) \sigma_{\gamma A \rightarrow A J/\psi}(-y) \quad (3)$$

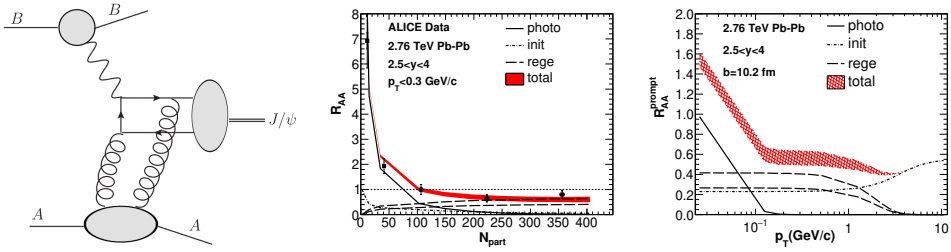


Figure 5. (Color online) Left panel is the schematic figure for photoproduction. The middle panel is J/ψ inclusive R_{AA} as a function of N_p in the extremely low p_T at 2.76 TeV Pb-Pb collisions. The right panel is the prompt R_{AA} as a function of p_T . These figures are cited from [12, 36].

As the cross section of photoproduction in Eq.(3) is proportional to the fourth of nuclear electric charges $\propto Z_e^4$, this photoproduction becomes important in AA collisions but negligible in the pp collisions. This additional contribution can enhance the nuclear modification factor R_{AA} in the semi-central and peripheral collisions in the extremely low p_T region, see the middle panel of Fig.5. Note that in the Ultra-peripheral collisions without hadronic collisions, the denominator of R_{AA} scaled from pp collisions approaches to zero, but the numerator is non-zero due to the photoproduction, which makes $R_{AA} \rightarrow +\infty$ at $N_p \rightarrow 0$. In the central collisions with a large number of binary collisions N_{coll} , hadroproduction increases significantly and photoproduction becomes negligible. The feature of photoproduction becomes more clear in the right panel of Fig.5. In $p_T > 5$ GeV/c of finally detected prompt J/ψ , primordial production becomes the main source. Regeneration becomes dominant in the middle and low p_T bins. In the extremely low $p_T < 0.1$ GeV/c, the photoproduction becomes larger than the hadroproduction, see the right panel of Fig.5.

2.4 B hadron decay

Final charmonium can come from the direct production and decay from higher excited state, and also the decay of B hadrons. This decay contribution from bottom flavor is labelled as “non-prompt” charmonium. The contributions of primordial production and regeneration is classified as the prompt part. In pp collisions, the fraction of non-prompt part in inclusive yield have been measured by experiments, fitted to be $f_B(p_T) = 0.04 + 0.023p_T/(GeV/c)$ for J/ψ and $f_B(p_T) = 0.11 + 0.022p_T/(GeV/c)$ for $\psi(2S)$. The momentum dependence of the $f_B(p_T)$ shows weak dependence on the colliding energies and the rapidities [37]. In AA collisions, the momentum distribution of bottom quarks will be modified by QGP when they move through the medium. The momentum shift of bottom quarks before hadronization changes the non-prompt yield at different p_T regions. This hot medium modification factor is called quenched factor $Q(p_T)$.

When we focus on prompt R_{AA} of J/ψ and $\psi(2S)$ at $p_T > 6.5$ GeV/c, lack of regeneration in this high p_T , primordially produced $\psi(2S)$ s are more easily dissociated by QGP compared with J/ψ , $R_{AA}^{\psi(2S)}/R_{AA}^{J/\psi}$ decreases with N_p , see the left panel of Fig.6.

After including the contribution of B hadron decay, J/ψ yield is less affected, as non-prompt J/ψ is less than the prompt ones due to J/ψ large binding energy. However, prompt $\psi(2S)$ s in the primordial production are strongly dissociated, their final inclusive yield is then dominated by the non-prompt part, see the second term of Eq.(4). $r_B = f_B/(1 - f_B)$ represents the ratio of non-prompt and prompt charmonium yields. The quench factor Q shows flat tendency with N_p in the region $100 < N_p < 400$ in experiments [36]. This makes inclusive

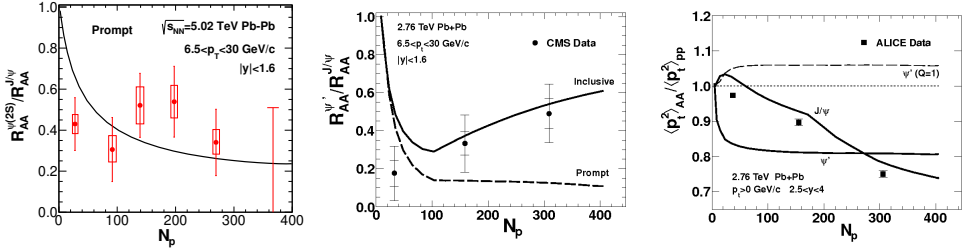


Figure 6. (Color online) The left panel is prompt $R_{AA}^{\psi(2S)}/R_{AA}^{J/\psi}$ in $6.5 < p_T < 30$ GeV/c in $\sqrt{s_{NN}} = 5.02$ TeV Pb-Pb collisions. The middle panel is prompt (dashed line) and inclusive (solid line) $R_{AA}^{\psi(2S)}/R_{AA}^{J/\psi}$ at $\sqrt{s_{NN}} = 2.76$ TeV. The decay rates for charmonia in left panel is updated compared with the middle panel. The right panel is $\langle p_T^2 \rangle_{AA}/\langle p_T^2 \rangle_{pp}$ of inclusive J/ψ and inclusive $\psi(2S)$. These figures are cited from AAAA.

$R_{AA}^{\psi(2S)}$ become flat. Inclusive $R_{AA}^{J/\psi}$ is dominated by the first term of Eq.(4) and decrease with N_p . Therefore, the inclusive $R_{AA}^{\psi(2S)}/R_{AA}^{J/\psi}$ decrease at first and then show clear increasing tendency at $100 < N_p < 400$, see the middle panel of Fig.6.

$$R_{AA}^{\text{inclusive}} = R_{AA}^{\text{prompt}} \frac{1}{1 + r_B} + \frac{r_B}{1 + r_B} Q \quad (4)$$

In the entire p_T region, regenerated J/ψ with small momentum will dominate the inclusive production, which suppress $\langle p_T^2 \rangle_{J/\psi}$. For inclusive $\psi(2S)$, its yield mainly consists of the non-prompt part from B hadron decay, as prompt part can barely survive from the QGP. This makes $\langle p_T^2 \rangle_{\psi(2S)}$ become flat with N_p , and is closely connected with the energy loss of bottom quarks, see the right panel of Fig.6.

3 Summary

In summary, we discuss different production mechanisms for both J/ψ and $\psi(2S)$ including primordial production, recombination of uncorrelated charm quarks in QGP and photoproduction from strong electromagnetic fields. Each of the production process dominates charmonium final yield in different p_T region because of their dynamical process. Transport models with all above ingredients can capture the main features of the experimental data of J/ψ and $\psi(2S)$ in both p-Pb and Pb-Pb collisions. These studies can provide clear picture of heavy quarkonium evolutions in the cooling deconfined medium. With the significant contribution of regeneration, hidden and open charm mesons are connected to each other. The space-time dependence of heavy quark diffusions also leave imprints on the heavy quarkonium yields and momentum distributions. The precise measurements about charmonium production in extremely low p_T also connects the hadroproduction from hadronic collisions with the photoproduction from electromagnetic fields which acts as one of the most important inputs in the studies of chiral/charged particle evolutions in heavy ion collisions. More explicit experimental data in small and large colliding systems for different charmonium states also provide promising opportunities to study the quantum effects of quarkonium states in the thermal medium.

Acknowledgements We thank Prof. Pengfei Zhuang for the help in above studies. B. Chen has been supported by NSFC Grant No. 11705125 and Sino-Germany (CSC-DAAD) Postdoc Scholarship.

References

- [1] T. Matsui and H. Satz, Phys. Lett. B **178**, 416 (1986).
- [2] L. Grandchamp and R. Rapp, Phys. Lett. B **523**, 60 (2001)
- [3] A. Andronic, P. Braun-Munzinger, K. Redlich and J. Stachel, Phys. Lett. B **571**, 36 (2003)
- [4] L. Yan, P. Zhuang and N. Xu, Phys. Rev. Lett. **97**, 232301 (2006)
- [5] B. Chen, K. Zhou and P. Zhuang, Phys. Rev. C **86**, 034906 (2012)
- [6] J. P. Blaizot, D. De Boni, P. Faccioli and G. Garberoglio, Nucl. Phys. A **946**, 49 (2016)
- [7] X. Yao and B. Müller, Phys. Rev. C **97**, no. 1, 014908 (2018) Erratum: [Phys. Rev. C **97**, no. 4, 049903 (2018)]
- [8] X. Yao and T. Mehen, arXiv:1811.07027 [hep-ph].
- [9] Y. Burnier, O. Kaczmarek and A. Rothkopf, Phys. Rev. Lett. **114**, no. 8, 082001 (2015)
- [10] H. Satz, J. Phys. G **32**, R25 (2006)
- [11] B. Chen, Phys. Rev. C **93**, 054905 (2016)
- [12] W. Shi, W. Zha and B. Chen, Phys. Lett. B **777**, 399 (2018)
- [13] A. Adare *et al.* [PHENIX Collaboration], Phys. Rev. Lett. **98**, 232301 (2007)
- [14] J. Adam *et al.* [ALICE Collaboration], Phys. Lett. B **766**, 212 (2017)
- [15] R. L. Thews, M. Schroedter and J. Rafelski, Phys. Rev. C **63**, 054905 (2001)
- [16] B. Chen, arXiv:1811.11393 [nucl-th].
- [17] A. Adare *et al.* [PHENIX Collaboration], Phys. Rev. Lett. **98**, 172301 (2007)
- [18] X. Yao and B. Müller, arXiv:1811.09644 [hep-ph].
- [19] B. Chen, Phys. Rev. C **95**, 034908 (2017)
- [20] X. Du and R. Rapp, Nucl. Phys. A **943**, 147 (2015)
- [21] D. E. Kharzeev, L. D. McLerran and H. J. Warringa, Nucl. Phys. A **803**, 227 (2008)
- [22] S. Klein and J. Nystrand, Phys. Rev. C **60**, 014903 (1999)
- [23] J. Adam *et al.* [ALICE Collaboration], Phys. Rev. Lett. **116**, no. 22, 222301 (2016)
- [24] B. Chen, T. Guo, Y. Liu and P. Zhuang, Phys. Lett. B **765**, 323 (2017)
- [25] K. J. Eskola, H. Paukkunen and C. A. Salgado, JHEP **0904**, 065 (2009)
- [26] X. Du and R. Rapp, arXiv:1808.10014 [nucl-th].
- [27] E. G. Ferreira, Phys. Lett. B **749**, 98 (2015)
- [28] B. Chen, X. Du and R. Rapp, Nucl. Part. Phys. Proc. **289-290**, 475 (2017)
- [29] J. Zhao and B. Chen, Phys. Lett. B **776**, 17 (2018)
- [30] M. He, R. J. Fries and R. Rapp, Phys. Rev. C **86**, 014903 (2012)
- [31] G. Baur, K. Hencken, D. Trautmann, S. Sadovsky and Y. Kharlov, Phys. Rept. **364**, 359 (2002)
- [32] V. A. Khoze, A. D. Martin and M. G. Ryskin, Eur. Phys. J. C **24**, 459 (2002)
- [33] G. M. Yu, Y. B. Cai, Y. D. Li and J. S. Wang, Phys. Rev. C **95**, no. 1, 014905 (2017) Addendum: [Phys. Rev. C **95**, no. 6, 069901 (2017)]
- [34] G. M. Yu, Y. C. Yu, Y. D. Li and J. S. Wang, Nucl. Phys. B **917**, 234 (2017)
- [35] E. Fermi, Z. Phys. **29**, 315 (1924).
- [36] B. Chen, C. Greiner, W. Shi, W. Zha and P. Zhuang, arXiv:1801.01677 [hep-ph].
- [37] T. Aaltonen *et al.* [CDF Collaboration], Phys. Rev. D **80**, 031103 (2009)